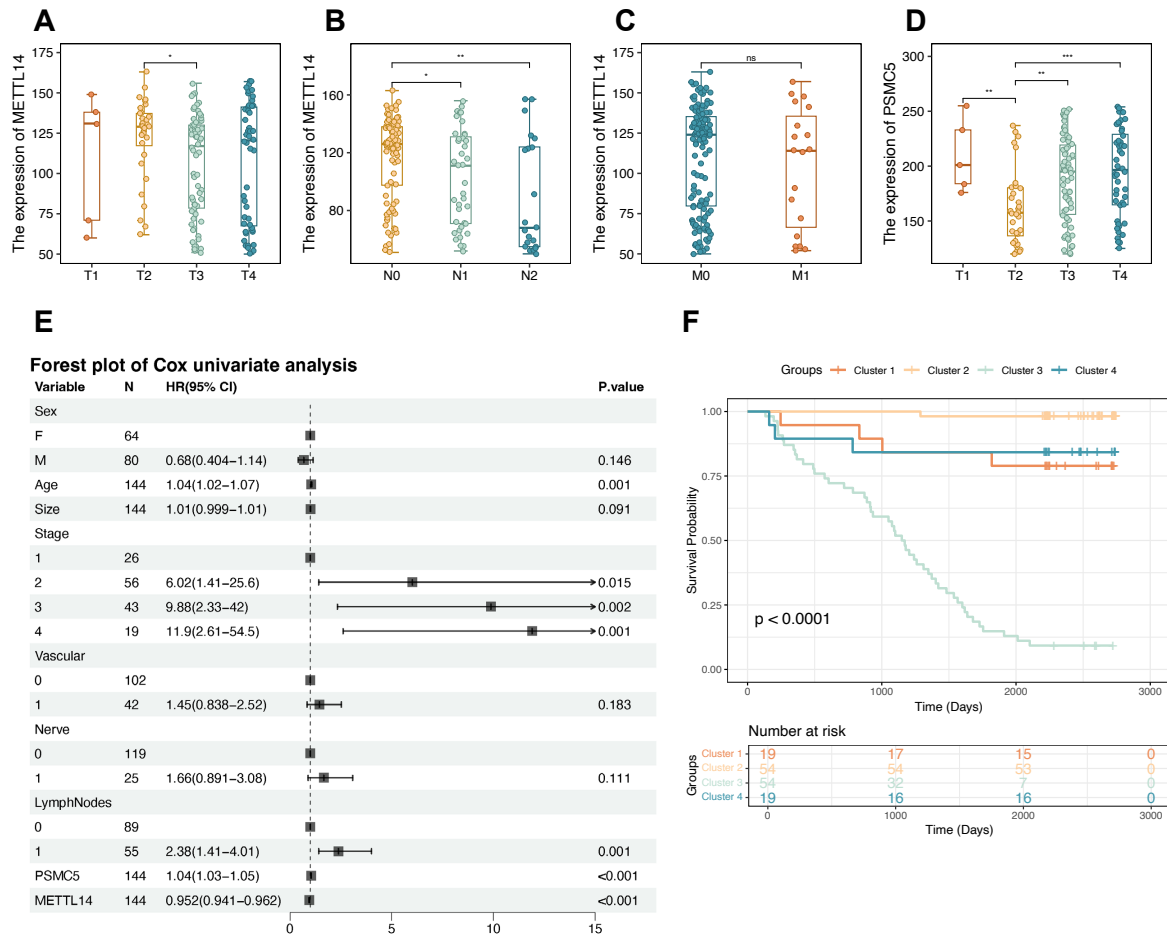


**Figure S1** (A) Kaplan-Meier survival curves for TCGA colorectal cancer patients stratified into four groups by combined PSMC5 and METTL14 expression. Cluster 1: PSMC5 low and METTL14 low. Cluster 2: PSMC5 low and METTL14 high. Cluster 3: PSMC5 high and METTL14 low. Cluster 4: PSMC5 high and METTL14 high. (B) GO Biological Process (BP)

term enrichment for differentially methylated mRNAs resulting from PSMC5 overexpression. (C) GO Molecular Function (MF) term enrichment for differentially methylated mRNAs associated with PSMC5 overexpression. (D) GO Cellular Component (CC) term enrichment for differentially methylated mRNAs associated with PSMC5 overexpression. (E) KEGG pathway enrichment analysis of differentially expressed mRNAs between the PSMC5-overexpression and NC groups following RNA sequencing. Statistical analysis: log-rank test for (A); hypergeometric test for enrichment for (B-E).



**Figure S2** (A) METTL14 IHC scores stratified by T stage (T1-T4). (B) METTL14 IHC scores stratified by N stage (N0-N2). (C) METTL14 IHC scores stratified by M stage (M0/M1). (D) PSMC5 IHC scores stratified by T stage (T1-T4). (E) Univariate Cox analysis for overall survival including clinicopathologic variables and IHC scores of PSMC5 and METTL14; forest plot displays HRs and 95% CIs. Statistical tests as in Fig. 2. (F) Kaplan-Meier survival curves for the institutional cohort stratified by combined PSMC5 and METTL14 immunohistochemical expression into four groups: Cluster 1, PSMC5 low/METTL14 low; Cluster 2, PSMC5 low/METTL14 high; Cluster 3, PSMC5 high/METTL14 low; and Cluster 4, PSMC5 high/METTL14 high. The number of patients at risk is shown below. Statistical analysis: Kruskal-Wallis test with multiple-comparison correction for (A, B, D); Wilcoxon

rank-sum test for (C); Wald test from Cox proportional hazards regression for (E); log-rank test for (F). \*P<0.05, \*\*P<0.01, \*\*\*P<0.001, \*\*\*\*P<0.0001, ns, not significant.

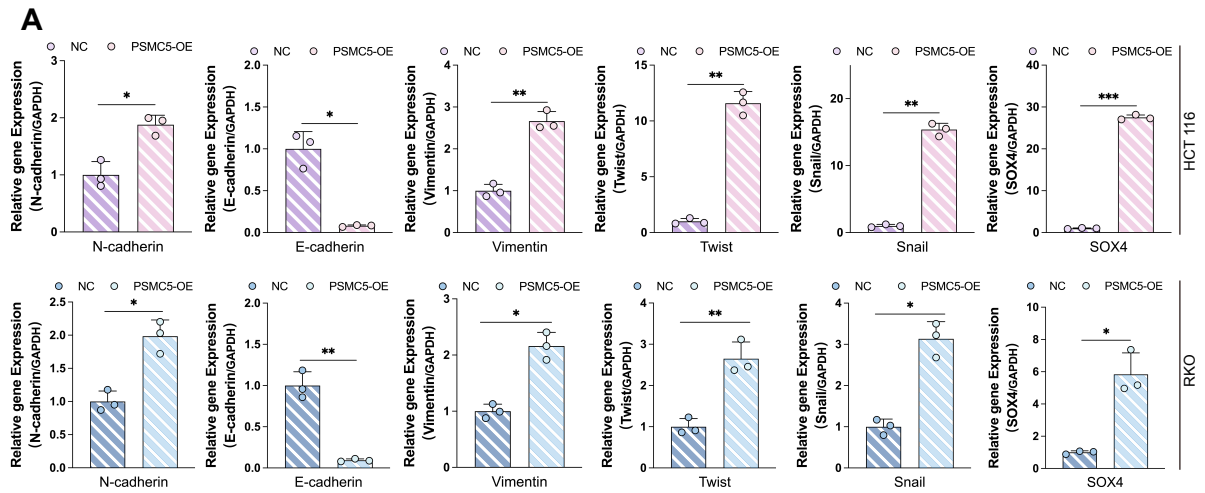


**Figure S3 (A)** qRT-PCR analysis of N-cadherin, E-cadherin, Vimentin, Twist, Snail, and SOX4 expression in HCT116 and RKO cells stably expressing control vector or PSMC5. Gene expression was normalized to GAPDH. Statistical analysis: unpaired two-tailed Student's t test. Data are presented as mean  $\pm$  SD from three independent biological replicates. \* $P < 0.05$ , \*\* $P < 0.01$ , \*\*\* $P < 0.001$ .

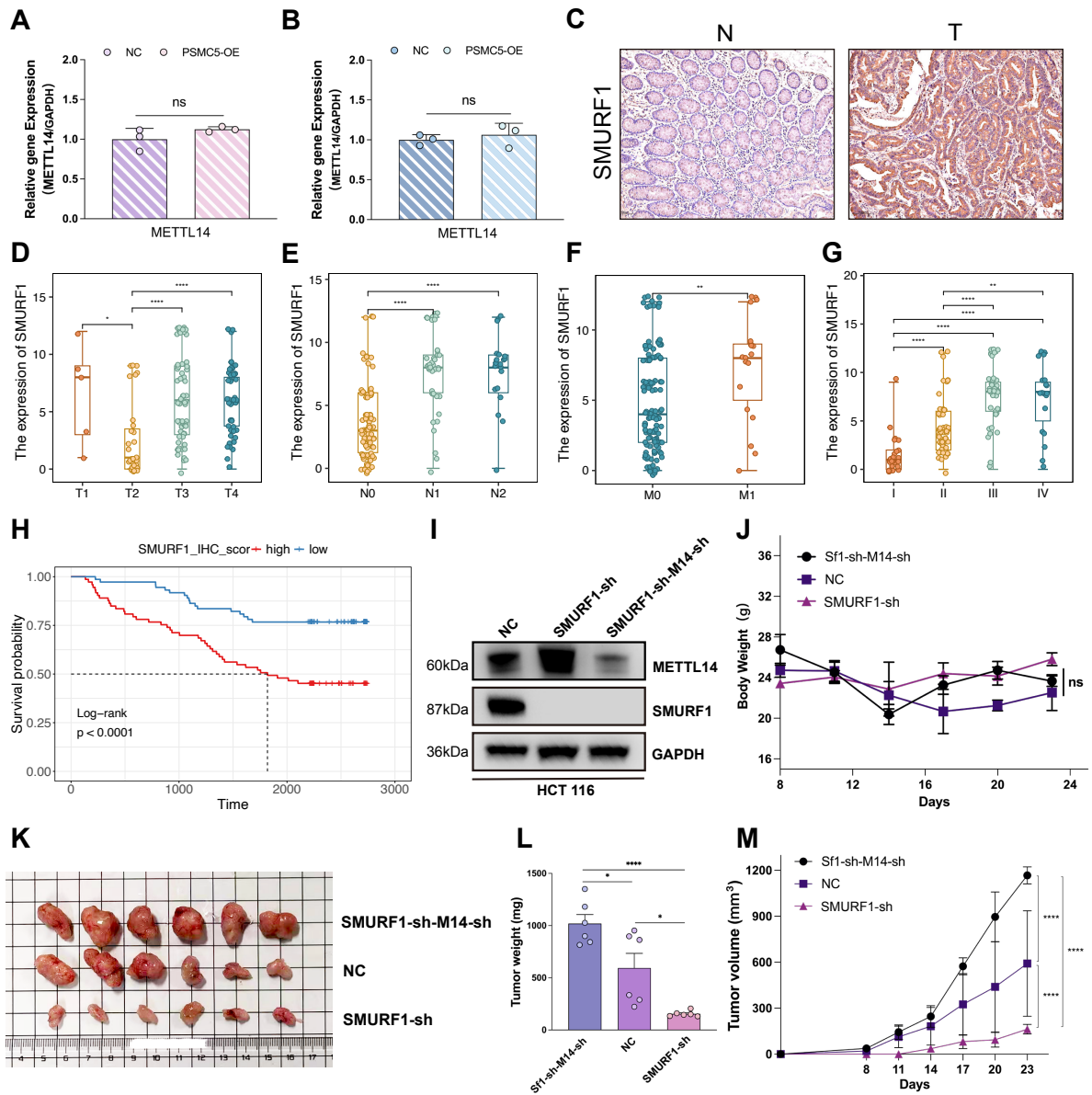


**Figure S4** (A-B) qRT-PCR analysis of METTL14 mRNA expression in HCT116 and RKO cells with lentivirus-mediated stable overexpression of PSMC5 or corresponding control cells. Gene expression was normalized to GAPDH. (C) Representative immunohistochemical staining of SMURF1 in normal colorectal mucosa (N) and colorectal tumor tissue (T). (D-G) Association of SMURF1 expression with clinicopathological characteristics of colorectal cancer, including T stage (D), N stage (E), M stage (F), and pathological stage (G). (H) Kaplan-Meier overall survival curves for colorectal cancer patients stratified by SMURF1

immunohistochemical score (high vs low). (I) Immunoblotting of METTL14 and SMURF1 in HCT116 cells from the NC, SMURF1-sh, and SMURF1-sh+METTL14-sh groups. GAPDH served as a loading control. (J) Body weight curves of mice in the NC, SMURF1-sh, and SMURF1-sh+METTL14-sh groups during the subcutaneous xenograft experiment. (K) Representative images of subcutaneous xenograft tumors excised from mice in the NC, SMURF1-sh, and SMURF1-sh+METTL14-sh groups. (L) Final tumor weights of subcutaneous xenografts from mice in the NC, SMURF1-sh, and SMURF1-sh+METTL14-sh groups at the endpoint of the experiment. (M) Tumor growth curves of subcutaneous xenografts formed by HCT116 cells in the NC, SMURF1-sh, and SMURF1-sh+METTL14-sh groups. Tumor volumes were recorded at the indicated time points. Statistical analysis: unpaired two-tailed Student's t test for (A, B); Kruskal-Wallis test with multiple-comparison correction for (D, E, G); Wilcoxon rank-sum test for (F); log-rank test for (H); two-way repeated-measures ANOVA with multiple-comparison correction for (J, M); one-way ANOVA with multiple-comparison correction for (L). Panels (C, I, K) show representative images. \* $P < 0.05$ , \*\* $P < 0.01$ , \*\*\* $P < 0.001$ , \*\*\*\* $P < 0.0001$ , ns, not significant.

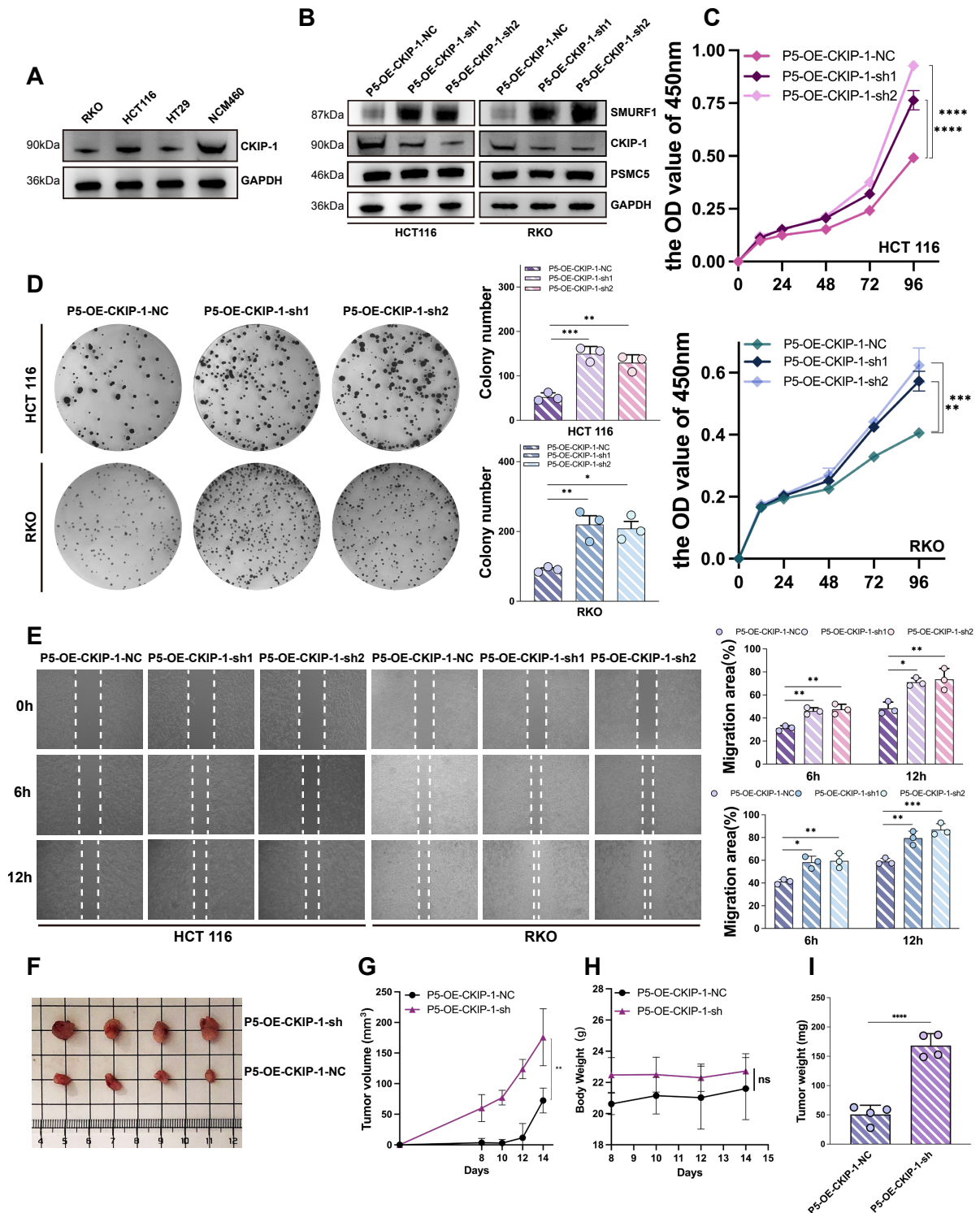


**Figure S5** (A) Immunoblotting of CKIP-1 in RKO, HCT116, HT29, and NCM460 cells. GAPDH served as a loading control. (B) Immunoblotting of SMURF1, CKIP-1, and PSMC5 in HCT116 and RKO cells from the P5-OE-CKIP-1-NC, P5-OE-CKIP-1-sh1, and P5-OE-CKIP-1-sh2 groups. GAPDH served as a loading control. (C) CCK-8 growth curves of

HCT116 and RKO cells in the indicated groups. (D) Representative colony-formation images and quantification in HCT116 and RKO cells from the indicated groups. (E) Wound-healing assays with quantification of migration area in HCT116 and RKO cells from the indicated groups. (F) Representative images of subcutaneous xenograft tumors excised from nude mice in the P5-OE-CKIP-1-NC and P5-OE-CKIP-1-sh groups. (G) Tumor growth curves of subcutaneous xenografts in the indicated groups. (H) Body weight curves of mice in the indicated groups during the xenograft experiment. (I) Final tumor weights of subcutaneous xenografts at the experimental endpoint. Data are presented as mean  $\pm$  SD. Statistical analysis: two-way repeated-measures ANOVA with Tukey's multiple-comparison test for (C, E, G, H); one-way ANOVA with Tukey's multiple-comparison test for (D); unpaired two-tailed Student's t test for (I). \*P<0.05, \*\*P<0.01, \*\*\*P<0.001, \*\*\*\*P<0.0001, ns, not significant.

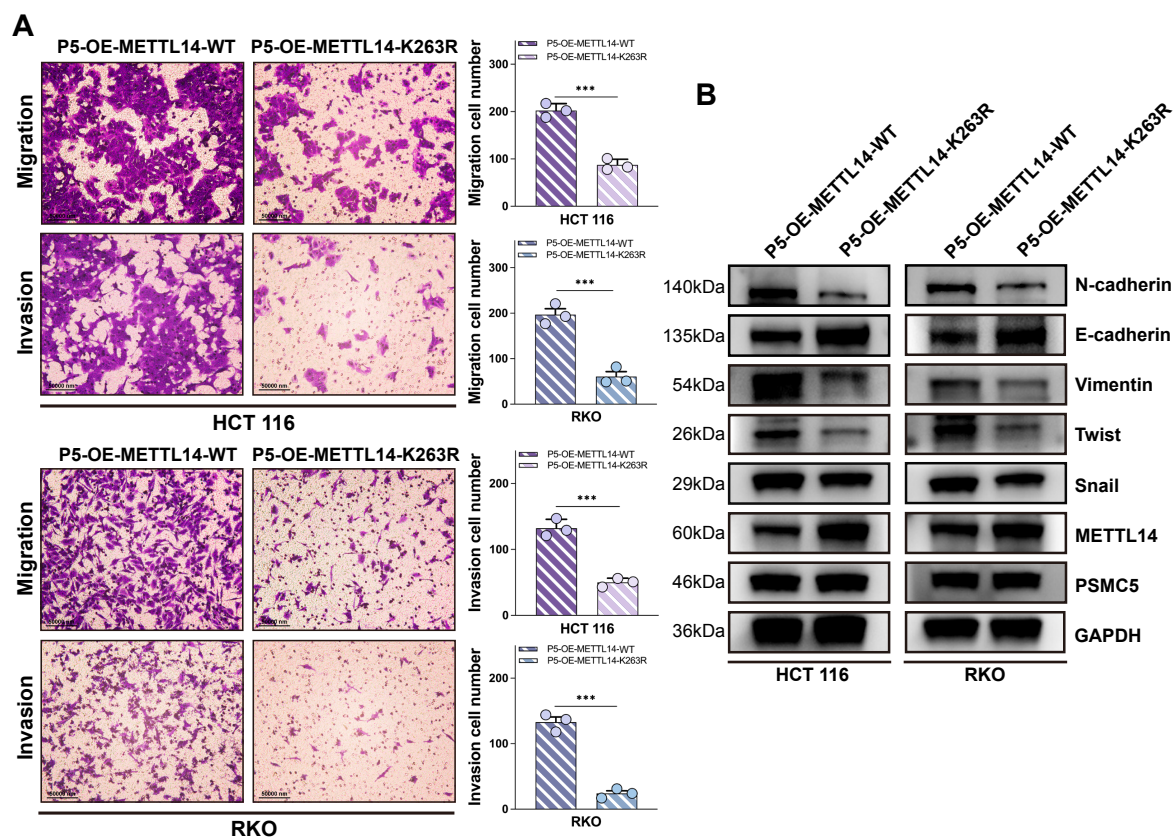


**Figure S6** (A) Transwell migration (without Matrigel) and invasion (with Matrigel) assays with representative images and quantification of migrated or invaded cells in HCT116 and RKO cells with stable PSMC5 overexpression, followed by transfection with METTL14-WT or METTL14-K263R plasmids. (B) Immunoblotting of EMT-related proteins (N-cadherin, E-cadherin, Vimentin, Twist, and Snail) together with METTL14 and PSMC5 in HCT116 and RKO cells with stable PSMC5 overexpression, followed by transfection with METTL14-WT or METTL14-K263R plasmids. GAPDH served as a loading control. Data are presented as mean  $\pm$  SD from three independent biological replicates. Statistical analysis: unpaired two-tailed Student's t test for the quantification in (A). Panel (B) shows representative immunoblot images. \* $P < 0.05$ , \*\* $P < 0.01$ , \*\*\* $P < 0.001$ .

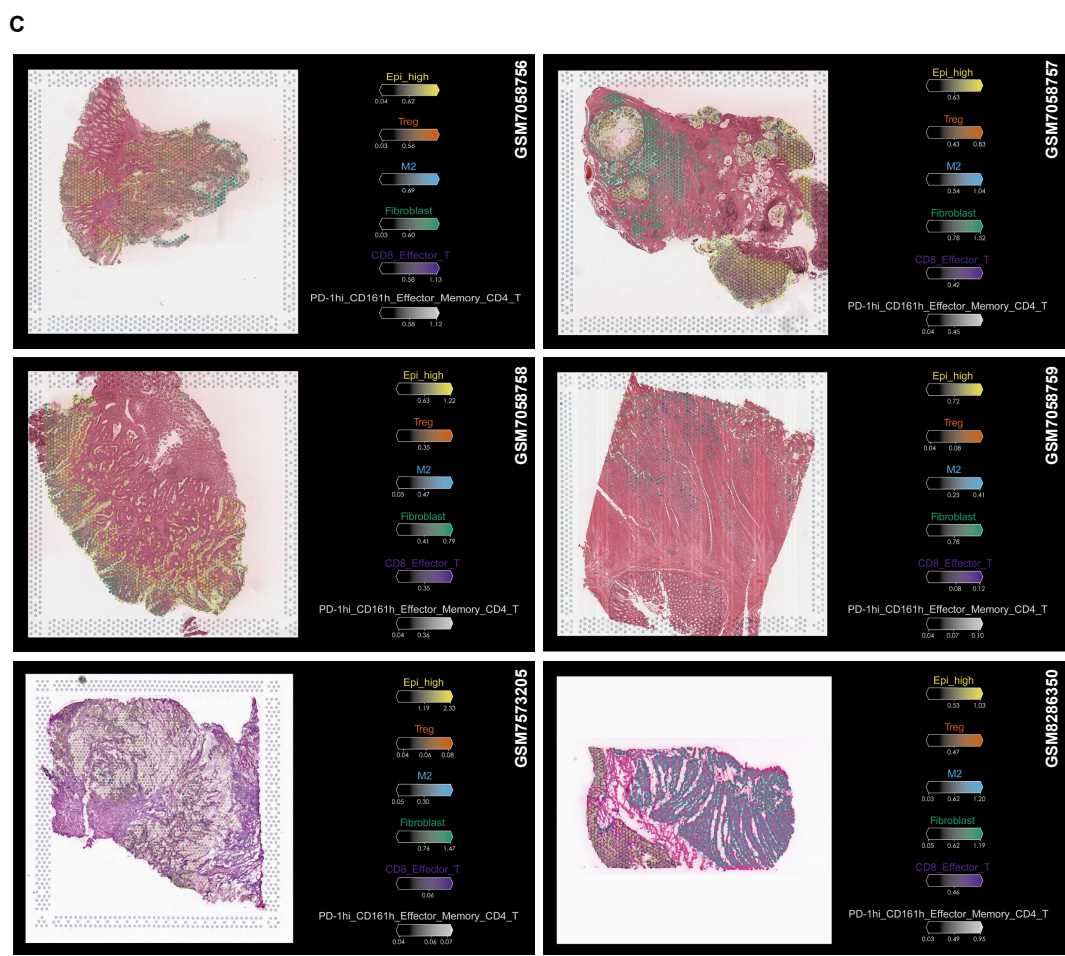
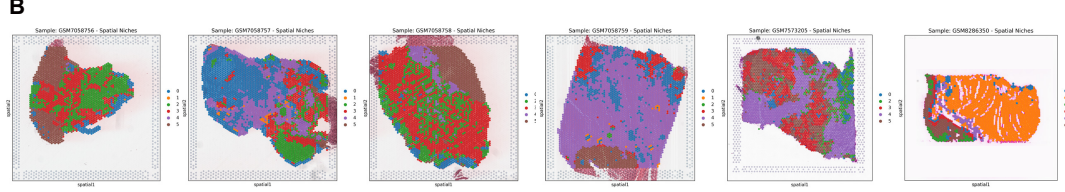
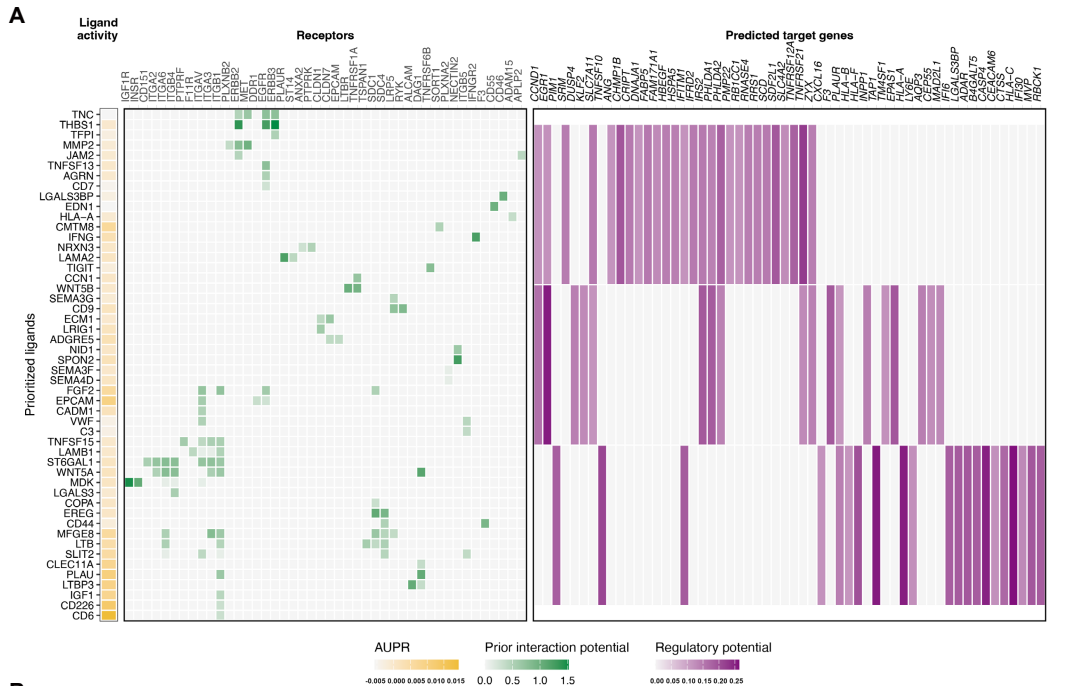


**Figure S7** (A) Extended ligand-receptor-target landscape corresponding to Figure 8E, showing ligand activity (AUPR), receptor connectivity and regulatory potential on downstream target genes. (B) Spatial transcriptomic maps of six tissue sections, including five colorectal cancer tumors (GSM7058756-GSM7058759; GSM7573205) and one normal colonic tissue (GSM8286350), showing spatial niche assignment across the tissue sections. (C) Spatial distribution maps of selected cellular programs and immune/stromal components across the six tissue sections, including PSMC5-high epithelial cells, Tregs, M2 macrophages, fibroblasts, CD8<sup>+</sup> effector T cells, and PD-1-high-CD161-high effector memory CD4<sup>+</sup> T cells.

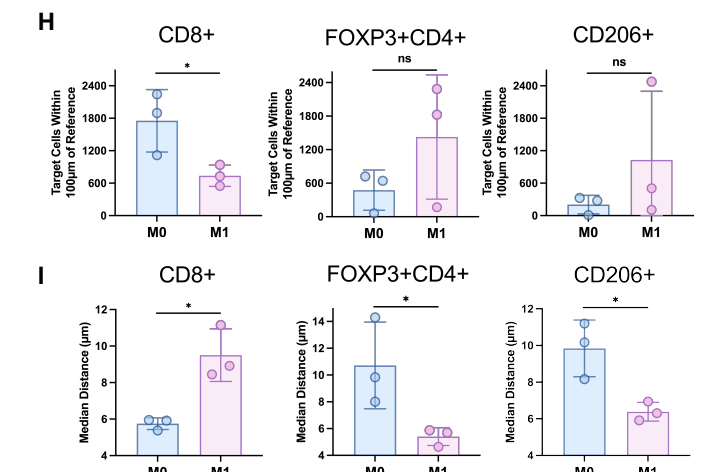
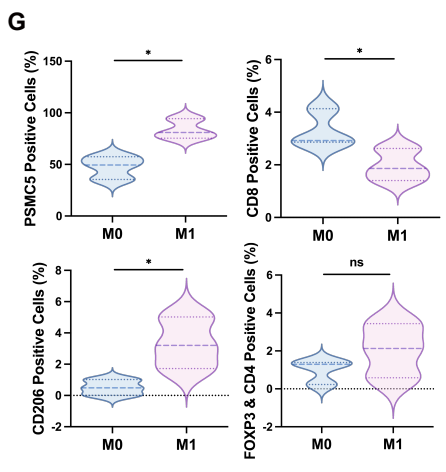
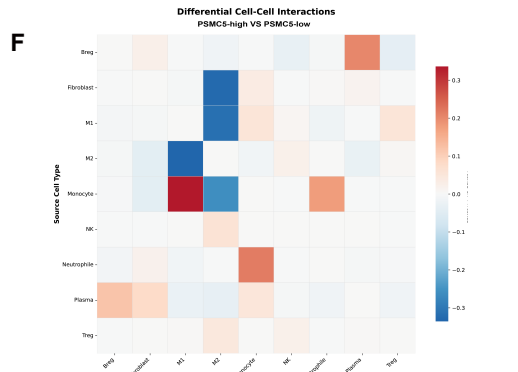
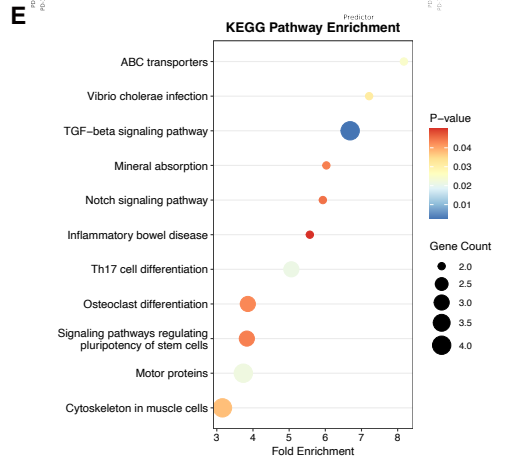
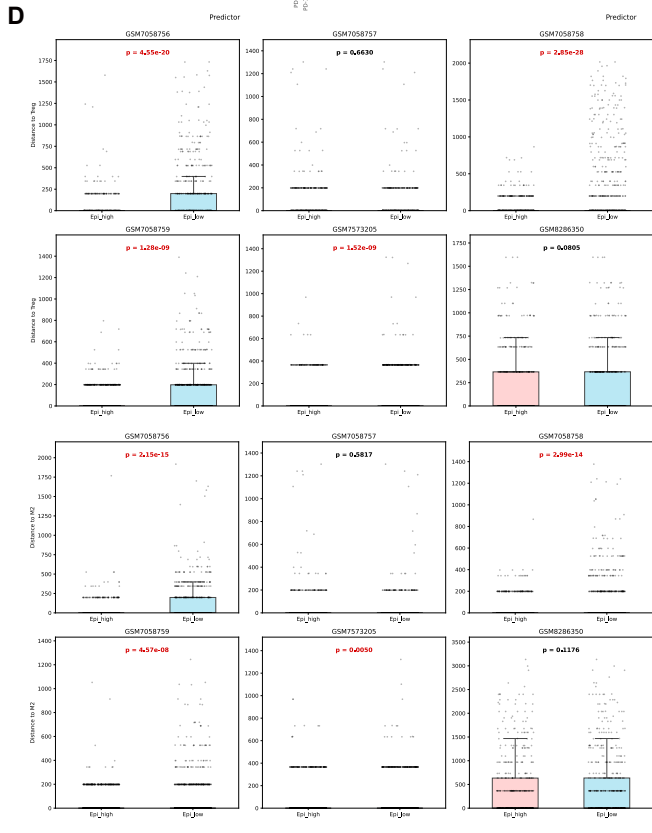
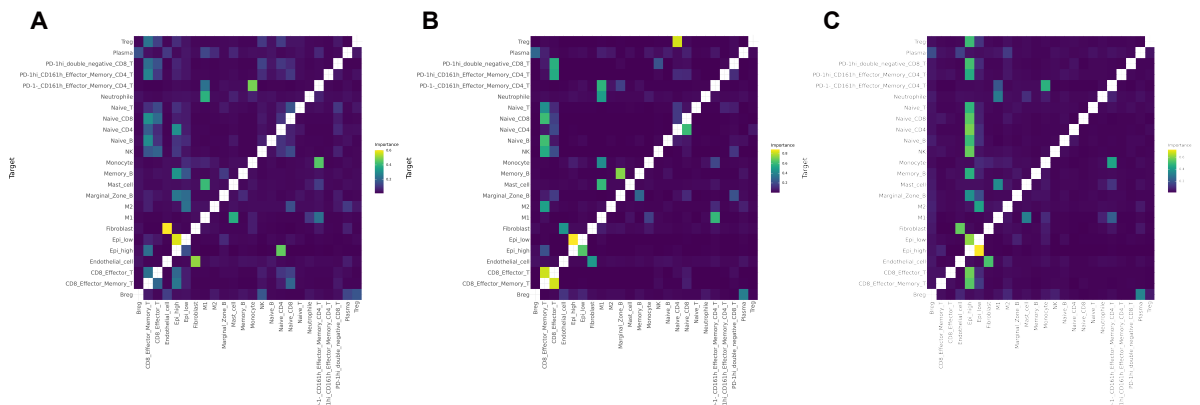


**Figure S8** (A) Within-spot interaction heatmap summarizing co-occurrence of predictor and target cell types in the same Visium spot. (B) Adjacent-spot interaction heatmap depicting co-localization of predictor cell types in the six neighboring spots around each target cell type. (C) Paraspot interaction heatmap quantifying co-localization of predictor and target cell types in spots beyond the immediate six neighbors, indicating long-range association patterns within the tumor microenvironment. (D) Section-wise comparison of the average Euclidean distance between PSMC5-high or PSMC5-low epithelial spots and the nearest Treg or M2 macrophage spot across colorectal cancer and normal colonic tissue sections. Cell-type-specific spots were defined as the top 30% spots for each signature. (E) KEGG pathway enrichment analysis of genes upregulated in the PSMC5-high epithelial subpopulation compared with the PSMC5-low epithelial subpopulation. Bubble size indicates gene count, and color represents the enrichment P value. (F) Differential interaction heatmap comparing PSMC5-high versus PSMC5-low regions. Colors indicate increased (red) or decreased (blue) spatial association between source and target cell types. (G) Quantification of PSMC5<sup>+</sup> cells, CD8<sup>+</sup> cells, CD206<sup>+</sup> cells, and FOXP3<sup>+</sup>CD4<sup>+</sup> cells in primary colorectal tumors without metastasis (M0) and with metastasis (M1). (H) Quantification of CD8<sup>+</sup>, FOXP3<sup>+</sup>CD4<sup>+</sup>, and CD206<sup>+</sup> cells within 100  $\mu$ m of the reference region in M0 and M1 primary tumors. (I) Median distance from the reference region to CD8<sup>+</sup>, FOXP3<sup>+</sup>CD4<sup>+</sup>, and CD206<sup>+</sup> cells in M0 and M1 primary tumors. Statistical analysis: hypergeometric test for (E); unpaired two-tailed Student's t test for (G-I). Data are presented as mean  $\pm$  SD. For (D), P values are shown in the corresponding panels. \*P<0.05, ns, not significant.

Variables	All patients (n = 146)	High (n = 73)	Low (n = 73)	p value
Age, n (%)				0.19
< 65	74 (51%)	33 (45%)	41 (56%)	
≥ 65	72 (49%)	40 (55%)	32 (44%)	
Gender, n (%)				0.18
Female	64 (44%)	36 (49%)	28 (38%)	
Male	82 (56%)	37 (51%)	45 (62%)	
Size, n (%)				0.12
< 10 cm <sup>3</sup>	51 (35%)	21 (29%)	30 (41%)	
≥ 10 cm <sup>3</sup>	95 (65%)	52 (71%)	43 (59%)	
T stage, n (%)				< 0.001
1	5 (3.4%)	3 (4.1%)	2 (2.7%)	
2	31 (21%)	5 (6.8%)	26 (36%)	
3	62 (42%)	36 (49%)	26 (36%)	
4	48 (33%)	29 (40%)	19 (26%)	
N stage, n (%)				0.024
0	86 (59%)	37 (51%)	49 (67%)	
1	39 (27%)	20 (27%)	19 (26%)	
2	21 (14%)	16 (22%)	5 (6.8%)	
M stage, n (%)				0.007
0	127 (87%)	58 (79%)	69 (95%)	
1	19 (13%)	15 (21%)	4 (5.5%)	
Stage, n (%)				< 0.001
I	26 (18%)	2 (2.7%)	24 (33%)	
II	57 (39%)	32 (44%)	25 (34%)	
III	44 (30%)	24 (33%)	20 (27%)	
IV	19 (13%)	15 (21%)	4 (5.5%)	
Vascular Invasion, n (%)				0.59
No	103 (71%)	50 (68%)	53 (73%)	
Yes	43 (29%)	23 (32%)	20 (27%)	
Nerve Invasion, n (%)				0.51
No	121 (83%)	59 (82%)	62 (85%)	
Yes	25 (17%)	14 (19%)	11 (15%)	
Lymph Node Status, n (%)				0.089
No	90 (62%)	40 (55%)	50 (68%)	
Yes	56 (38%)	33 (45%)	23 (32%)	

**Table S1.** Clinicopathological features associated with PSMC5 expression in colorectal cancer patients. P values were calculated using Fisher's exact test.

Variables	All patients (n = 146)	High (n = 73)	Low (n = 73)	p value
Age, n (%)				0.51
< 65	74 (51%)	39 (53%)	35 (48%)	
≥ 65	72 (49%)	34 (47%)	38 (52%)	
Gender, n (%)				0.10
Female	64 (44%)	27 (37%)	37 (51%)	
Male	82 (56%)	46 (63%)	36 (49%)	
Size, n (%)				0.39
< 10 cm <sup>3</sup>	51 (35%)	28 (38%)	23 (32%)	
≥ 10 cm <sup>3</sup>	95 (65%)	45 (62%)	50 (68%)	
T stage, n (%)				0.047
1	5 (3.4%)	3 (4.1%)	2 (2.7%)	
2	31 (21%)	22 (30%)	9 (12%)	
3	62 (42%)	26 (36%)	36 (49%)	
4	48 (33%)	22 (30%)	26 (36%)	
N stage, n (%)				0.008
0	86 (59%)	52 (71%)	34 (47%)	
1	39 (27%)	15 (21%)	24 (33%)	
2	21 (14%)	6 (8.2%)	15 (21%)	
M stage, n (%)				0.22
0	127 (87%)	66 (90%)	61 (84%)	
1	19 (13%)	7 (9.6%)	12 (16%)	
Stage, n (%)				0.001
I	26 (18%)	21 (29%)	5 (6.8%)	
II	57 (39%)	30 (41%)	27 (37%)	
III	44 (30%)	15 (21%)	29 (40%)	
IV	19 (13%)	7 (9.6%)	12 (16%)	
Vascular Invasion, n (%)				0.86
No	103 (71%)	52 (71%)	51 (70%)	
Yes	43 (29%)	21 (29%)	22 (30%)	
Nerve Invasion, n (%)				0.12
No	121 (83%)	64 (88%)	57 (78%)	
Yes	25 (17%)	9 (12%)	16 (22%)	
Lymph Node Status, n (%)				0.006
No	90 (62%)	53 (73%)	37 (51%)	
Yes	56 (38%)	20 (27%)	36 (49%)	

**Table S2.** Clinicopathological features associated with METTL14 expression in colorectal cancer patients. P values were calculated using Fisher's exact test.

Variables	All patients (n = 146)	High (n = 73)	Low (n = 73)	p value
Age, n (%)				0.51
< 65	74 (51%)	35 (48%)	39 (53%)	
≥ 65	72 (49%)	38 (52%)	34 (47%)	
Gender, n (%)				0.74
Female	64 (44%)	33 (45%)	31 (42%)	
Male	82 (56%)	40 (55%)	42 (58%)	
Size, n (%)				0.22
< 10 cm <sup>3</sup>	51 (35%)	22 (30%)	29 (40%)	
≥ 10 cm <sup>3</sup>	95 (65%)	51 (70%)	44 (60%)	
T stage, n (%)				<0.001
1	5 (3.4%)	3 (4.1%)	2 (2.7%)	
2	31 (21%)	6 (8.2%)	25 (34%)	
3	62 (42%)	34 (47%)	28 (38%)	
4	48 (33%)	30 (41%)	18 (25%)	
N stage, n (%)				<0.001
0	86 (59%)	23 (32%)	63 (86%)	
1	39 (27%)	32 (44%)	7 (9.6%)	
2	21 (14%)	18 (25%)	3 (4.1%)	
M stage, n (%)				0.027
0	127 (87%)	59 (81%)	68 (93%)	
1	19 (13%)	14 (19%)	5 (6.8%)	
Stage, n (%)				<0.001
I	26 (18%)	1 (1.4%)	25 (34%)	
II	57 (39%)	21 (29%)	36 (49%)	
III	44 (30%)	37 (51%)	7 (9.6%)	
IV	19 (13%)	14 (19%)	5 (6.8%)	
Vascular Invasion, n (%)				0.1
No	103 (71%)	47 (64%)	56 (77%)	
Yes	43 (29%)	26 (36%)	17 (23%)	
Nerve Invasion, n (%)				0.83
No	121 (83%)	60 (82%)	61 (84%)	
Yes	25 (17%)	13 (18%)	12 (16%)	
Lymph Node Status, n (%)				<0.001
No	90 (62%)	27 (37%)	63 (86%)	
Yes	56 (38%)	46 (63%)	10 (14%)	

**Table S3.** Clinicopathological features associated with SMURF1 expression in colorectal cancer patients. P values were calculated using Fisher's exact test.

#### Antibodies used for western blot

Primary antibodies included PSMC5 (ab178681), SMURF1 (ab300408), METTL14 (26158-1-AP), N-cadherin (A19083), E-cadherin (ab231303), Snail (13099-1-AP), Twist (25465-1-AP), Vimentin (10366-1-AP), PLEKHO1 (24883-1-AP), GAPDH (60004-1-Ig), Ubiquitin (80992-1-RR), HA tag (51064-2-AP), FLAG tag (66008-4-Ig), MYC tag (60003-2-Ig), normal rabbit IgG isotype control (98136-1-RR) and Anti-Ubiquitin K11 linkage (MABS107-I).

Secondary antibodies were HRP-conjugated goat anti-mouse IgG (SA00001-1), HRP-conjugated goat anti-rabbit IgG (SA00001-2), and Universal type anti-heavy chain + light chain secondary antibody (M21008).

**Table S4.** Sequences of primers used for qRT-PCR.

METTL14-F	GGGGTTGGACCTTGGAAGAG
METTL14-R	CCCATGAGGCAGTG TTCCTT
N-cadherin-F	TGGAGCCTGATGCCATCAAG
N-cadherin-R	GAGCTGTGGGGTCATTGTCA
Vimentin-F	GGACCAGCTAACCAACGACA
Vimentin-R	AAGGTCAAGACGTGCCAGAG
Twist-F	GTCCGCAGTCTTACGAGGAG
Twist-R	GCCAGCTTGAGGGTCTGAAT
Snail-F	GAGGACAGTGGGAAAGGCTC
Snail-R	TGGAGATCCTTGGCCTCAGA
SOX4-F	GTCCCACTCCTCCTCCTCCT
SOX4-R	AGCCGGGCTCGAAGTTAAAA
E-cadherin-F	TTGAAGATTGCACCGGTCGA
E-cadherin-R	TCTGTAGGTGGAGTCCCAGG
GAPDH-F	GATTTGGTCGTATTGGGCGC
GAPDH-R	TTCCCGTTCTCAGCCTTGAC

Graphical abstract citation

Created in BioRender. Zhang, E. (2026) <https://BioRender.com/hs8awlt>